ISSN 1063-7826, Semiconductors, 2019, Vol. 53, No. 6, pp. 833–837. © Pleiades Publishing, Ltd., 2019.
Russian Text © The Author(s), 2019, published in Fizika i Tekhnika Poluprovodnikov, 2019, Vol. 53, No. 6, pp. 844–849.

PHYSICS OF SEMICONDUCTOR DEVICES

Trends in Reverse-Current Change in Tunnel MIS Diodes with Calcium Fluoride on Si(111) Upon the Formation of an Extra Oxide Layer

A. G. Banshchikov[a], Yu. Yu. Illarionov[a,b], M. I. Vexler[a,*], S. Wachter[b], and N. S. Sokolov[a]

[a] *Ioffe Institute, St. Petersburg, 194021 Russia*
[b] *Vienna University of Technology, Vienna, A-1040 Austria*
**e-mail: vexler@mail.ioffe.ru*

Received January 10, 2019; revised January 18, 2019; accepted January 18, 2019

Abstract—The currents flowing in metal–CaF_2–*n*-Si and metal–SiO_2–CaF_2–*n*-Si structures with the same (about 1.5 nm) fluoride thickness are compared in the reverse-bias mode. It is revealed that the current in the case of a two-layer dielectric can be notably higher within a certain voltage range. Such unexpected behavior is associated with the coexistence of both electron and hole components of the current as well as with the configuration of the SiO_2–CaF_2 barrier through which tunneling occurs. The results of measurements and explanatory simulation data are presented.

DOI: 10.1134/S1063782619060034

1. INTRODUCTION

Calcium fluoride (CaF_2) is a promising crystalline dielectric material for silicon devices [1], which, in particular, can serve as a gate insulator in field-effect transistors of various designs. At the same time, for preliminary study of the properties of CaF_2 layers, metal–insulator–semiconductor (MIS) structures in the reverse bias mode, which most closely corresponds to the conditions implemented in transistors, are traditionally used.

A significant advantage of fluoride is a high quality of its interface with silicon as compared with the case of amorphous insulators. However, in practice, the thickness of fluoride films is often insufficiently homogeneous. Therefore, sometimes one deposits another dielectric layer over CaF_2, usually, silicon dioxide (SiO_2). In this case, the addition of the oxide provides "smoothing" of the surface. The methods of forming a SiO_2 layer on CaF_2 may be different (for example, the authors of [2] carried out "additional oxidation" after the growth of CaF_2). Broadly speaking, the resulting system can be considered as a structure with a two-layer dielectric; however, unlike better known cases of high-k materials above a SiO_2 sublayer (for example, [3]), here the role of the sublayer is assigned to fluoride, while SiO_2 occurs "above" (see the inset in Fig. 1).

This study is devoted to analyzing the features of the behavior of reverse-biased metal–CaF_2–*n*-Si (111) structures with ultrathin epitaxial fluoride films (the nominal thickness is 6–7 monolayers, i.e., ~2 nm, but with fluctuations taken into account, it is effectively ~1.5 nm). Before depositing the metal, an extra SiO_2 layer is sometimes created so that a metal–SiO_2–CaF_2–*n*-Si system with a double insulator is obtained. The specific problem lies in clarifying the nature of variations in the tunneling current in the

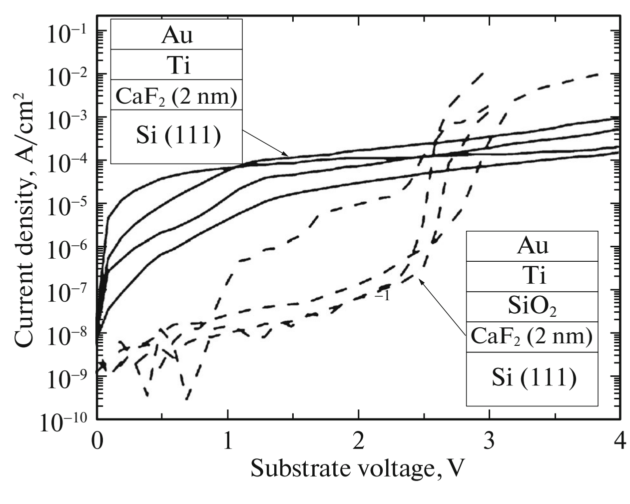

Fig. 1. Comparison of the experimental *I*–*V* characteristics of the metal–SiO_2–CaF_2–Si and metal–CaF_2–Si MIS structures with the same fluoride thickness (for several samples). At relatively high voltages, the current in the case of a two-layer barrier unexpectedly turns out to be higher.

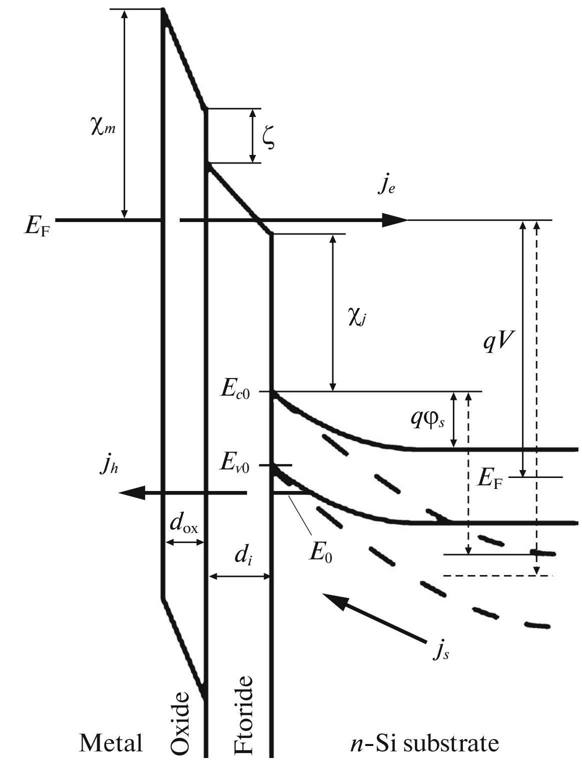

Fig. 2. Band diagram of the structure with fluoride and oxide. The profile of the bands in Si corresponds to a situation close to equilibrium (solid lines) and strong non-equilibrium (dotted line)—in the inset to Fig. 4, these two situations correspond to segments 1 and 2, respectively.

reverse-bias mode with the addition of an oxide layer. Intuitively, it is natural to foresee that SiO_2 increases the film resistance, i.e., the current always decreases at any given bias *V*, but, as it turns out, the situation is more complicated.

2. SAMPLES WITH CaF_2 AND SiO_2–CaF_2 FILMS

The samples under study represented two-electrode structures. The key technological stage of their fabrication was the formation of dielectric layers on moderately doped *n*-type silicon substrates (the concentration $N_D \sim 10^{16}$ cm^{-3}) with the crystallographic orientation (111).

The growth of fluoride films with an average thickness of 1.5–2.0 nm was carried out by molecular-beam epitaxy. In this case, the main point was the use of relatively low (~250°C) growth temperatures, which made it possible to minimize the number of triangular pinholes typical for fluoride formed at high temperature [2].

Certain CaF_2 films were covered with a dioxide layer by ion sputtering. Its thickness was not strictly set and amounted to units of nanometers. It should be noted that, as was clarified in the process of study, the behavior of the samples after long-term storage (several weeks or more) in a laboratory without specially deposited SiO_2 became qualitatively similar to the behavior of the structures with a two-layer insulator (it is likely that additional oxidation due to available air took place).

We deposited metal contacts consisting of 5 nm Ti and 30 nm Au also by ion sputtering.

3. MEASUREMENTS. PRINCIPAL FEATURE OF *I–V* CHARACTERISTICS

We measured the steady-state characteristics of samples under a positive substrate bias *V* with respect to the metal. As already noted, in the MIS structures with calcium fluoride as well as with other dielectrics, it is the reverse-bias mode that is of principal practical interest, i.e., with such a polarity at which an inversion layer, which is the hole one in this case, is induced at the dielectric–substrate interface. The problem was to compare the behavior of the structures only with a fluoride layer and with an additional oxide layer at the indicated polarity.

It was found that the measured *I–V* characteristics often have the following trend. At relatively low voltages *V* up to ~2–3 V, the current through a double dielectric layer (SiO_2–CaF_2) is significantly lower than in the sample with one CaF_2 layer; however, as *V* increases, the current level in the structure with SiO_2–CaF_2 is higher approximately by an order of magnitude (Fig. 1). If the decrease in the current in the initial portion of the metal–SiO_2–CaF_2–*n*-Si structure in comparison with a single-layer structure is taken as natural and induces no questions, an increase in the current in a certain region of higher voltages seems to be at first glance paradoxical and requires explanation.

4. AUXILLIARY MODELING

To achieve an understanding of the situation, we carried out auxiliary semi-quantitative modeling.

We highlight its most important moments relevant with respect to the systems under study. The tunneling current $j = j_e + j_h$ consists of hole (from the level E_0 in the valence band of Si into metal, Fig. 2) and electron (the metal–Si conduction band) components, which are the currents of minority and majority charge carriers: $j_{\min} = j_h$ and $j_{\mathrm{maj}} = j_e$. For simplicity, we assume that electron transfer takes place mainly in the vicinity of kt (kt is the thermal energy) of the Fermi energy E_F, then the known expression [4] for the current j_e takes the form:

$$j_e = 4\pi q m_0 (kt)^2 h^{-3} T_e(E_F). \tag{1}$$

Holes give the main contribution to the field in the dielectric due to the smallness of N_D, while their energy level with respect to the bottom of the Si valence band at the interface can be written as

$$E_0 = \frac{55}{32}\sqrt[3]{\frac{9}{11}}\left(\frac{q^2\hbar N_s}{\varepsilon_0\varepsilon_s\sqrt{m_z}}\right)^{2/3}, \quad N_s = \frac{\varepsilon_0\varepsilon_i F_i}{q}, \tag{2}$$

i.e., according to the formula from [5] by neglecting the charge of donors (here N_s is the two-dimensional density of holes, and m_z is their mass). Correspondingly, the hole current is found as

$$j_h = qN_s(E_0/h)T_h(E_{v0} - E_0). \tag{3}$$

In the formulas for the current components, the probabilities of tunneling are written somewhat differently for j_e and j_h:

$$T_e(E) = \exp\left[-2\hbar^{-1}\left(\int\sqrt{2m_{ei}(E_{ci}(z) + m_0m_{ei}^{-1}\Delta E - E)}dz + \int\sqrt{2m_{e\text{ox}}(E_{e\text{ox}}(z) + m_0m_{e\text{ox}}^{-1}\Delta E - E)}dz\right)\right], \tag{4}$$

$$T_h(E) = \exp\left[-2\hbar^{-1}\left(\int\sqrt{2m_{ei}(E_{ci}(z) - E)}dz + \int\sqrt{2m_{h\text{ox}}(E - E_{v\text{ox}}(z))}dz\right)\right]. \tag{5}$$

The difference consists in the fact that, for tunneling from the metal to the conduction band, the presence of a large in magnitude electron transverse wave vector (case Si(111) orientation) is effectively taken into account for which we introduce the term with

$$\Delta E = \Delta E_0 \exp[-(E_F - E_{c0})/E_s], \tag{6}$$

where $\Delta E_0 = 2.44$ eV, and $E_s = 1$ eV. This formula was tested by us in [6]. The barrier heights are marked in Fig. 2. The values of the parameters: effective masses in the oxide are $m_{e\text{ox}} = 0.42m_0$ and $m_{h\text{ox}} = 0.33m_0$; in fluoride: $m_{ei} = 1.0m_0$, the discontinuities of bands: $\xi = 0.77$ eV, $\chi_i = 2.38$ eV [7]; the permittivities $\varepsilon_{\text{ox}} = 3.9$ (SiO_2), $\varepsilon_i = 8.43$ (CaF_2), and $\varepsilon_s = 11.9$ (Si). The tunneling through CaF_2 is always implemented through the upper barrier $E_{ci}(z)$.

5. CAUSES OF GROWTH IN THE CURRENT WITH THE ADDITION OF SiO_2

In our opinion, the increase in the current when adding the oxide can be due to two not mutually exclusive reasons.

First, as we noted previously, when a double-layer barrier is deformed, it can become more tunnel-transparent as compared with a single-layer barrier [8]. If for the sake of simplicity we neglect the band bending $q\varphi_s$ in Si and do not consider the component j_h, it is easy to see (inset in Fig. 3) that, at high voltages V, only the oxide part of the tunnel barrier "works", where the effective mass is smaller. In Fig. 3, we plot the curves $j(V)$ calculated disregarding the bending; it turns out that the indicated barrier deformation in a certain range of changes of parameters could explain the effect.

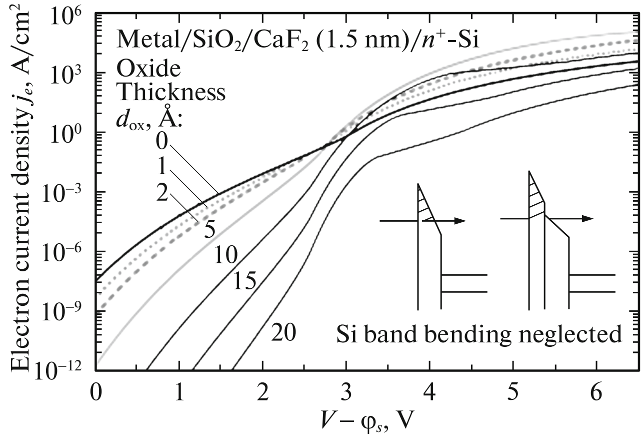

Fig. 3. Calculated electron tunneling current in the metal–CaF_2–n-Si and metal–SiO_2–CaF_2–n-Si MIS structures for the case of disregarding the bending of bands in silicon. For relatively high voltages, higher currents are predicted in the two-layer case, which is associated with the deformation of the tunnel barrier shown in the inset (one of the possible explanations of the experimental result in Fig. 1).

Second, it is known that a slowdown in current growth in the MIS structures with voltage can be observed in the depletion–inversion modes [9]. This is owing to a deficiency in minority charge carriers, which are created by thermal generation or photogeneration in the Si bulk, supplied to the interface (the current j_s), and are used to provide the leakage current j_h (Fig. 2). The voltage across the dielectric at the given V is established to provide the balance $j_s = j_{\min}$. The I–V characteristic consists of two segments (see inset in Fig. 4): up to a certain bias, the field in the dielectric and the current increase sharply (in this case, $q\varphi_s$ is small, see also Fig. 2) and then there arises a "plateau" (where $q\varphi_s$ grows). If the bulk–interface current j_s is formed by thermal generation, it varies from zero to a certain value of j_{s0} like in the reverse-biased p–n junction: the relation $j_s < j_{s0}$ corresponds to the current increase, and $j_s = j_{s0}$—to the plateau. To estimate the value of the current on the plateau

$$j_{\text{plateau}} = j_{e,\text{plateau}}(F_i, F_{\text{ox}}, d_i, d_{\text{ox}}) + j_{s0},$$

$$F_{i|\text{ox}} = F_{i|\text{ox}}\big|_{j_h = j_{s0}}, \tag{7}$$

the values of the fields F_i, F_{ox} ($= F_i\varepsilon_i/\varepsilon_{\text{ox}}$) in dielectrics corresponding to the condition $j_{s0} = j_h$ should first be found by setting a certain fixed value of j_{s0} (for example, 10^{-9} A/cm^2). Then the current j_e can be calculated with previously found fields. Correspondingly, there appears the possibility to track how the plateau current varies at a set fluoride thickness (for example, d_i = 1.5 nm) and oxide thickness d_{ox} varying from zero to several nanometers. Since the dependences of the components of currents on fields are complex and dif-

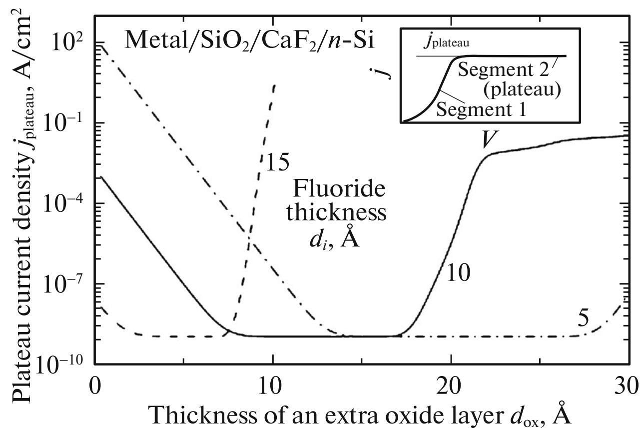

Fig. 4. Calculated current through the metal–SiO_2–CaF_2–*n*-Si reverse-biased MIS structure on the plateau; the segments of the initial increase in current and plateau are marked in the inset. The thermal-generation current is set equal to 10^{-9} A/cm^2, the qualitative picture is independent of this value. The current of the plateau in a certain oxide-thickness range can be higher than without the oxide (one of the possible explanations of the result in Fig. 1).

ferent for j_e and j_h, the plateau current greatly depends on the parameters of materials.

The predicted dependence of the current $j_{plateau}(d_{ox})$ in the metal–SiO_2–CaF_2–*n*-Si system is nonmonotonic (Fig. 4). There are both regions of current decrease with thickness and growth regions. The current drop at small SiO_2 thicknesses is explained by the fact that there are no strong changes in the field, and the probability T_e decreases with thickness. A further sharp increase in $j_{plateau}$ in a certain thickness range is associated with the beginning of the field growth in dielectrics (it is clear that, in the direct-tunneling mode for a thicker oxide, the same thermal current j_{s0} is able to support a stronger field). Therefore, as d_{ox} grows, electrons are injected with increased fields of F_{ox} and F_i, and, which is more important, with higher energies, and such a process is characterized by a much higher probability T_e as the difference $E_F - E_{c0}$ grows, since the role of the factor ΔE decreases. As can be seen, the appearance of the oxide (the replacement of $d_{ox} = 0$ for a certain finite value) may well lead to an increase in the $j_{plateau}$ current.

6. EXPERIMENTAL DATA AND INTERPRETATION

It follows from the preceding section that, to identify the first mechanism explaining an increase in current by the deformation of the barrier in the case of SiO_2–CaF_2, conditions with a small bending of bands in silicon are more convenient, i.e., segment 1 (marked in the inset to Fig. 4). At the same time, to implement the second mechanism, within which an excess in current is associated with the coexistence of electron and hole components in the case of a lack of minority charge carriers, it is exactly segment 2 that is necessary.

The observed variants of the measured *I*–*V* characteristics ("+" on Si) are specified in Figs. 5a and 5b. It should be noted that intentionally oxidized samples were used [8] as bilayer structures in Fig. 5a and those that had undergone natural additional oxidation were used in Fig. 5b; though, this detailization is not so important because the effect was not related to the method of oxide formation. As can have already seen in Fig. 1, the current in the metal–SiO_2–CaF_2–Si structures at high voltages proves to be higher than in metal–CaF_2–Si structures with fluoride of the same thickness. There were cases, when the current in a two-layer structure became higher in the ascending portion (Fig. 5a), and other cases, where the intersection point in the *I*–*V* characteristics was located on the current plateau (Fig. 5b). The difference between the samples may be caused by a difference in the rate of thermal-carrier generation, as a result of which certain samples are in mode 1 at the same value of *V*, and some, in mode 2. It should be noted that we used the logarithmic scale in Fig. 5a (unlike Fig. 5b); i.e., there is no stabilization to the right of $V = 1$ V as it may seem.

Correspondingly, it can be concluded that the mechanism related to deformation of the barrier (shown in Fig. 3), and the mechanism associated with the behavior features of the current of minority carriers (Fig. 4) are real. Be that as it may, an unexpected effect of increasing the current in the case of a two-layer film as compared with a single-layer one can be quite simply explained. Of course, all this only qualitatively explained an increase in current, since the degree of conservation of the transverse wave vector in a real structure is not clear.

It is evident that similar features can appear for other combinations of dielectrics, and if the deformation mechanism of the tunneling barrier is real only in the case of different materials, then, an increase in the current plateau due to changes in the relation between j_h and j_e, in principle, is not excluded even with thickening of a homogeneous layer.

7. ADDITIONAL NOTES

One technical detail irrelevant as applied to the *I*–*V* characteristics in Fig. 5, but significant in the practical work with many similar samples, should be noted. In the case of complex MIS structures with new insulating materials (where active thermal generation occurs also at the interface instead of only in the Si bulk), segment 2 on the *I*–*V* characteristics does not always have a distinct plateau as in the schematic inset in Figs. 4 and 5b. It happens that the transition from segment 1 to segment to 2 manifests itself only in a

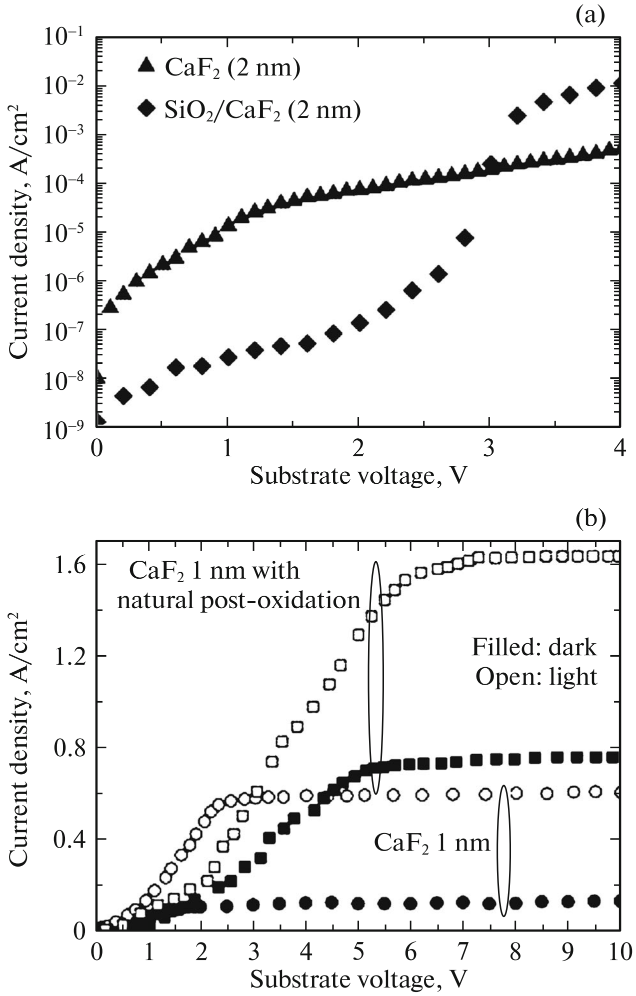

Fig. 5. Comparison of the measured *I*–*V* characteristics of the metal–SiO_2–CaF_2–*n*-Si and metal–CaF_2–*n*-Si MIS structures: (a) intentionally oxidized samples, (b) samples that underwent natural oxidation. Solid lines—in the dark, and dotted lines (Fig. 5b)—during irradiation. At low voltages, the current through the two-layer dielectric is lower and, at high voltages, is higher. A change in the trend can occur both in the portion of the current rise (segment 1, Fig. 5a) and on the plateau (segment 2, Fig. 5b).

change that is likely not even particularly obvious in the *I*–*V*-characteristic slope.

In such cases, to assign a certain voltage to segment 1 or 2, it is the nature of the response of the structure to external irradiation with a photon energy exceeding the band gap of Si [10] that is of importance. The photosensitivity on segment 2 is much stronger because the bending of bands decreases in the semiconductor during irradiation due to the generation of minority carriers, and the reserve of such a decrease is large in segment 2 and small in segment 1.

Although segment demarcation in Fig. 5b is clear, the corresponding figure is supplemented with curves recorded under irradiation: the regions of weak and strong response to light are singled out. In this case, the photosensitivity in Fig. 5a was almost absent both in the leftmost part of the curve in Fig. 5b (essentially the entire shown portion of the *I*–*V* characteristic in Fig. 5a refers to segment 1, while segment 2, likely, might appear at higher *V*, when the sample is already damaged).

8. CONCLUSIONS

In the study, it was found that the addition of an oxide layer to a fluoride layer in a MIS tunnel structure leads to a decrease in the through current only in the range of relatively small voltages, while at high biases, on the contrary, there is an increase in the current. The possible explanations for such behavior taking into account the tunnel-barrier deformation as well as the coexistence of electron and hole components of the current are proposed. It is likely that both of these mechanisms act jointly.

This result should be considered when implementing the oxidation of fluoride films which is practiced to increase their resistance (in this case, the advantages of the crystalline interface are preserved). In addition, it can be considered as an interesting feature of tunnel MIS structures in general, since a similar behavior is hypothetically possible also at different combinations of dielectric materials than were considered in this study.

REFERENCES

1. M. Sugiyama and M. Oshima, Microelectron. J. **27**, 361 (1996).
2. S. Watanabe, M. Maeda, T. Sugisaki, and K. Tsutsui, Jpn. J. Appl. Phys. B **44**, 2637 (2005).
3. A. Huang, X. Zhang, Y. Li, M. Wang, and Z. Xiao, J. Appl. Phys. **122**, 195702 (2017).
4. E. M. Vogel, K. Z. Ahmed, B. Hornung, W. K. Henson, P. L. McLarty, G. Lucovsky, J. R. Hauser, and J. J. Wortman, IEEE Trans. Electron Dev. **45**, 1350 (1998).
5. A. F. Shulekin, M. I. Vexler, and H. Zimmermann, Semicond. Sci. Technol. **14**, 470 (1999).
6. S. E. Tyaginov, Yu. Yu. Illarionov, M. I. Vexler, M. Bina, J. Cervenka, J. Franco, B. Kaczer, and T. Grasser, J. Comput. Electron. **13**, 733 (2014).
7. Ph. Avouris and R. Wolkow, Appl. Phys. Lett. **55**, 1074 (1989).
8. Yu. Yu. Illarionov, A. G. Banshchikov, N. S. Sokolov, S. Wachter, and M. I. Veksler, Tech. Phys. **44** (12) (2018, in press).
9. S. M. Sze, *Physics of Semiconductor Devices* (Wiley, New York, 1981), Vol. 2, Chap. 9.
10. B. C. Hsu, C.-Y. Liu, W.-T. Liu, and H.-L. Chen, IEEE Trans. Electron Dev. **48**, 1747 (2001).

Translated by V. Bukhanov